Ⓔ

THE ASSEMBLY OF MASSIVE GALAXIES FROM NEAR-INFRARED OBSERVATIONS OF THE HUBBLE DEEP FIELD–SOUTH

A. Fontana,[1] I. Donnarumma,[1] E. Vanzella,[2,3] E. Giallongo,[1] N. Menci,[1] M. Nonino,[4]
P. Saracco,[5] S. Cristiani,[4] S. D'Odorico,[2] and F. Poli[1]
Received 2003 April 29; accepted 2003 July 17; published 2003 August 8

ABSTRACT

We use a deep $K_{AB} \leq 25$ galaxy sample in the Hubble Deep Field–South to trace the evolution of the cosmological stellar mass density from $z \simeq 0.5$ to $z \simeq 3$. We find clear evidence for a decrease of the average stellar mass density at high redshift, $2 \leq z \leq 3.5$, that is $15^{+25}_{-5}\%$ of the local value, 2 times higher than observed in the Hubble Deep Field–North. To take into account for the selection effects, we define a homogeneous subsample of galaxies with $10^{10}\, M_\odot \leq M_* \leq 10^{11}\, M_\odot$: in this sample, the mass density at $z > 2$ is $20^{+20}_{-5}\%$ of the local value. In the mass-limited subsample at $z > 2$, the fraction of passively fading galaxies is at most 25%, although they can contribute up to about 40% of the stellar mass density. On the other hand, star-forming galaxies at $z > 2$ form stars with an average specific rate of at least $\langle \dot{M}/M_* \rangle \simeq 4 \times 10^{-10}\ \mathrm{yr}^{-1}$, 3 times higher than the $z \leq 1$ value. This implies that UV-bright star-forming galaxies are substancial contributors to the rise of the stellar mass density with cosmic time. Although these results are globally consistent with Λ-CDM scenarios, the present rendition of semianalytic models fails to match the stellar mass density produced by more massive galaxies present at $z > 2$.

Subject headings: galaxies: evolution — galaxies: formation — galaxies: high-redshift

On-line material: color figures

1. INTRODUCTION

The most distinctive features of current theories of galaxy formation is the mechanism relating the assembly of the galactic potential wells (mainly determined by the dark matter content) to the build-up of the stellar population contained therein. Hierarchical theories of galaxy formation are characterized by a gradual enrichment of the star content of galaxies driven by their progressive growth through merging events. This implies an appreciable antievolution with z of the galactic stellar mass distribution, in particular for the massive galaxies, which, in such theories, have assembled relatively late.

Recent surveys have started to directly follow this process by estimating the stellar mass content of galaxies up to $z \sim 3$, either from detailed spectral analysis (Kauffmann et al. 2003) or from multiwavelength imaging observations (Giallongo et al. 1998; Brinchmann & Ellis 2000, hereafter BE00; Drory et al. 2001; Cole et al. 2001; Papovich et al. 2001, hereafter P01; Shapley et al. 2001; Dickinson et al. 2003, hereafter D03). The latter technique relies on multicolor broadband imaging—extended into the near-IR range—to estimate the stellar content by a comparison with spectral synthesis models. In this work we present the results that this technique yields when applied to the Hubble Deep Field–South (HDF-S) data at $0 < z < 3.2$ and compare them with the predictions of a semianalytic model in a Λ-dominated cosmology ($\Omega_m = 0.3$, $\Omega_\Lambda = 0.7$, and $H_0 = 70$ km s^{-1} Mpc^{-1}). A Salpeter initial mass function (IMF) is used in the Letter.

2. STELLAR MASSES FROM THE HDF-S DATA

The data that we use here are the results of the HDF-S multiwavelength deep imaging survey, which combines the *Hubble Space Telescope* optical data (Casertano et al. 2000) in the F300W, F450W, F606W, and F814W filters (hereafter U, B, V, and I) and the ultradeep VLT-ISAAC IR images in the Js, H, and Ks filters (the AB photometric system has been used throughout the Letter). The latter data, which are in common with the FIRES survey (Labbé et al. 2003; Franx et al. 2003), have typical exposure times of about 30 hr in each filter and were reduced and analyzed following the recipes of Vanzella et al. (2001) and Fontana et al. (2000, F00). An a posteriori correlation with the FIRES data shows a good agreement in the measured colors and noise estimates. We will use here the $K_{AB} \leq 25$ sample, where the signal-to-noise ratio is larger than 5, although our results rely essentially on the brighter objects. The sample contains 302 objects, 59 with spectroscopic redshift (Vanzella et al. 2002; Sawicki & Mallen-Ornelas 2003), that were used to verify that the accuracy of photometric redshifts is comparable to our results in the HDF-N.

In this catalog, we have estimated the stellar content of the HDF-S galaxies by a comparison with spectral synthesis models, following the recipes of previous works (Giallongo et al. 1998; BE00; F00; P01; D03), In particular, we have adopted the same parameterization: we have used the Bruzual & Charlot (1993) GISSEL 2000 code with Salpeter IMF, a range of exponentially declining star formation histories with timescales from $\tau = 0.1$ Gyr to $\tau = \infty$ Gyr, metallicities of $Z/Z_\odot = 0.02, 0.2, 1, 2.5$, and dust extinction $[0 \leq E(B-V) \leq 1]$. As in F00, we have also added a set of multiple-burst models, although only 5% of the objects turned out to be fitted by such models. The best-fitting model to the observed multiwavelength distribution (at the spectroscopic or photometric redshifts) is used to estimate the stellar mass M_* (which includes a correction for the recycled fraction) in each galaxy sample. As in P01, we tested both a SMC-like extinction curve (used as at-

[1] INAF, Osservatorio Astronomico di Roma, via Frascati 33, I-00040 Monteporzio, Italy.
[2] European Southern Observatory, Karl-Schwarzschild-Strasse 2, D-85748 Garching, Germany.
[3] INAF, Osservatorio Astronomico di Padova, Vicolo dell'Osservatorio 2, I-35122 Padova, Italy.
[4] INAF, Osservatorio Astronomico di Trieste, via G. B. Tiepolo 11, I-34131 Trieste, Italy.
[5] INAF, Osservatorio Astronomico di Brera, via E. Bianchi, 46 Merate, Italy.

tenuation) and a Calzetti et al. (2000) one. With the latter, the mass estimates are slightly smaller than SMC (25% on average), since the Calzetti curve yields lower fitted ages than the SMC, with an unpleasant fraction of 40% of galaxies with ages ≤ 0.1 Gyr at any z. The fits based on the Calzetti curve have also typically poorer χ^2 and would be preferred only for 20% (40%) of the $z \leq 2$ ($z > 2$) galaxies. Given the uncertainties in the dust treatment, and because of these systematic differences, we present both results separately, with more emphasis on the SMC-based results.

The uncertainties involved in this approach, due to the degeneracy among the input models as well as from photometric noise and from the use of photometric redshifts, have been estimated on the basis of the reduced χ^2, computed as in F00. The 1 σ confidence levels on the fitted parameters (such as mass, age, and star formation rate) have been obtained by scanning the model grid and retaining only the models that have $\chi^2 \leq \chi^2_{\text{best-fit}} + 1$. Prior to this, as in P01, we have rescaled the noise in bright objects in order to have $\chi^2_{\text{best-fit}} = 1$ The scan is performed either at fixed redshift (for objects with known spectroscopic redshift) or allowing the models to move around the best-fitting photometric redshifts.

In the following, we shall also make use of a "maximal mass" estimate to provide upper limits to the estimated stellar mass of each object, being still broadly consistent with the observed colors. We have first assumed that all the UV light is due to a recent starburst with minimal M_*/L ratio (obtained from a model with constant SFR, $Z = 0.2\ Z_\odot$, age = 0.2 Gyr) and computed its contribution to the K-band flux. Then, we have used a maximally old stellar population to convert the residual K band to M_*.

We remind that *IR-selected samples do not strictly correspond to mass-selected ones*. At any z, the faint side of the sample is biased against the detection of high-mass, low-luminosity objects, i.e., old, passively evolving, or highly extincted galaxies. Because of the uncertainties in the modeling of such objects, it is difficult to define a clear selection threshold. We plot in Figure 1 two selection curves, such that objects above the lines should be used to compute statistics that require mass-selected samples, although several objects of lower mass (i.e., star-forming galaxies with lower M_*/L) are detected. In one case we use a GISSEL 2000 dust-free passively evolving model ignited by an instantaneous burst of subsolar metallicity at $z = 18$ (*short-dashed line*); in another we use the more realistic model of Le Borgne & Rocca-Volmerange (2002, *long-dashed line*) that reproduces the colors of local E0 and that self-consistently includes the effects of finite burst duration, dust absorption, and metallicity evolution.

Our sample is definitely incomplete below these curves, and reasonably complete above, except for strongly obscured sources. In the following we will roughly adopt a completeness limit at $M = 10^{10}\ M_\odot$ at $z > 2$.

3. THE GALAXY STELLAR MASS DENSITY

Figure 1 shows the best-fit stellar mass derived for each galaxy in the HDF-S, at the corresponding redshifts. We note that, due to the small volume sampled by the HDF-S, the most massive objects have typical masses around $10^{11}\ M_\odot$ even at low-to-intermediate z, nearly a factor of 10 smaller than those obtained by larger area surveys. We note, however, that several objects above $M_* \simeq 10^{10}\ M_\odot$ exist above $z = 2$, the most massive being an extremely red object at $z_{\text{phot}} \simeq 2.8$ with $M_* \simeq 2 \times 10^{11}\ M_\odot$, which is better described in a separate paper (Saracco et al. 2003).
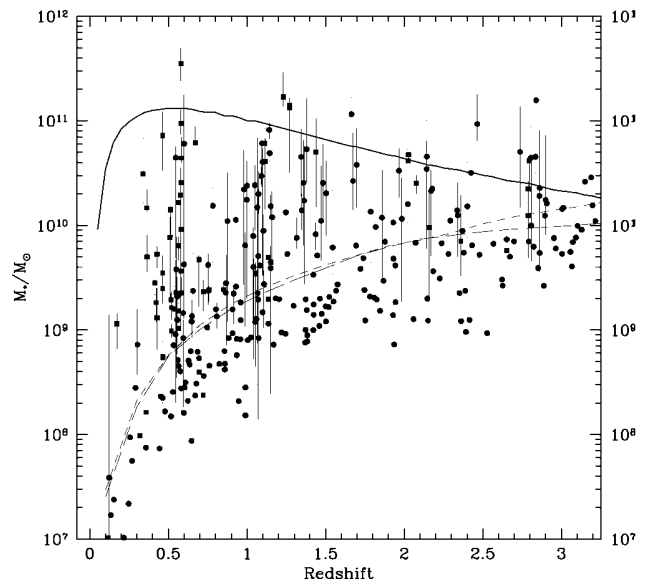

FIG. 1.—Galaxy stellar masses in the HDF-S sample as a function of z. The points represent the "best-fit" estimates with SMC extinction curve of the stellar masses (squares are objects with spectroscopic z). Error bars show the 1 σ confidence level and are computed including both the SMC and the Calzetti extinction laws. The solid line has been computed from the CDM hierarchical models of Menci et al. (2002), such that about three objects are expected from $z = 0$ to $z = 3$. The short- and long-dashed lines represent two possible selection curves above which the sample is mass complete (see text for details). [*See the electronic edition of the Journal for a color version of this figure.*]

To check whether the evolution of the more massive galaxies in our sample is consistent with theoretical expectations, we have used the CDM models of Menci et al. (2002) to compute a threshold M_{th}^* defined such that one expects one galaxy above it (in the area sampled by the HDF-S observations) per unit redshift (Fig. 1, *solid line*). The curve follows the growth of the high-mass tail of the galaxy stellar mass function on a hierarchical scenario. Quantitatively, we find 17 galaxies above the threshold, against the expected three, first evidence that the high-mass tail of the galaxy stellar mass function is not adequately followed by present CDM models.

In the upper panel of Figure 2, we present the stellar mass density $\rho_*(z)$ computed from our whole sample with the standard $1/V_{\text{max}}$ estimator, corrected to account for incompleteness analogously to D03. We plot separately both the SMC and the Calzetti-based estimates. We also plot other available estimates of the stellar mass density as obtained from other surveys at $z \simeq 1$ (BE00; Cohen 2002), and most notably with the HDF-N results (D03), that have similar depth, size, and adopted technique. While the evolution at $z \leq 1.5$ in both HDFs is consistent within errors (and with other surveys), it is remarkable to observe that we find in the HDF-S a stellar mass density at $2 \leq z \leq 3.2$ that is about 2 times higher than in HDF-N.

At face value, the observed values of $\rho_*(z)$ witness a fast increase of the stellar mass density from 7% to 15% of the local (with an upper limit of 40%) at $z \geq 2$ to about unity at $z \leq 1$, i.e., in a relatively short amount of cosmic time. Following Cole et al. (2001) and D03, we have compared the observed evolution with available theoretical expectations. We use an analytic fit to the global star formation rate of Steidel et al. (1999), with two different dust extinctions [$E(B-V) = 0, 0.15$] and our CDM hierarchical model; both the CDM model and the integrated contribution of the global star formation rate with a reasonable dust extinction provide a good fit to the data. However, a clean interpretation of the HDF-S data must take
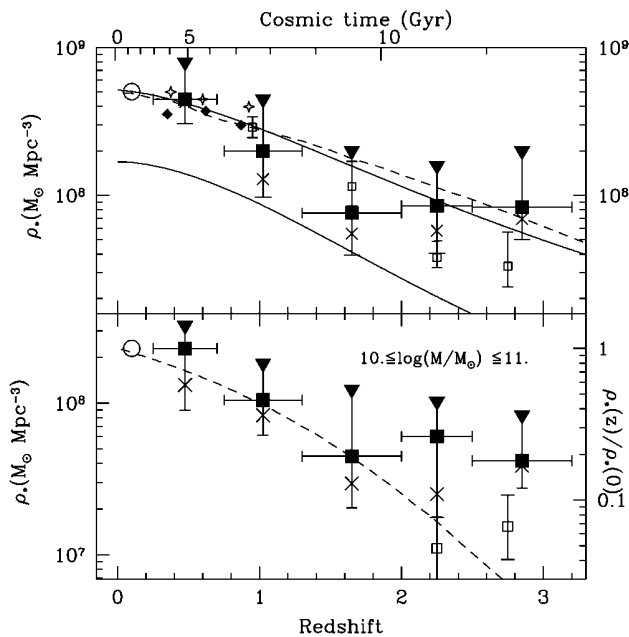
FIG. 2.—Evolution of the stellar mass density as a function of redshift. *Upper panel*: Observed values as estimated from the present work (*solid squares*, SMC; *crosses*, Calzetti) and from similar surveys: Dickinson et al. (2003, *open squares*), Cohen (2002, *open triangles*), Brinchmann & Ellis (2000, *filled triangles*), and Cole et al. (2001, *circle*). Upper error bars are extended at the level obtained from the "maximal mass" model; lower error bars represent the number counts noise. The two solid lines are the result of integrating the cosmic star formation history with and without dust (*upper and lower curves, respectively*). The dashed line is the result of the CDM hierarchical model of Menci et al. (2002). *Lower panel*: Symbols and curves as in above, but computed only in the fixed mass interval 10^{10} $M_\odot \leq M_* \leq 10^{11}$ $M_\odot$. [*See the electronic edition of the Journal for a color version of this figure.*]
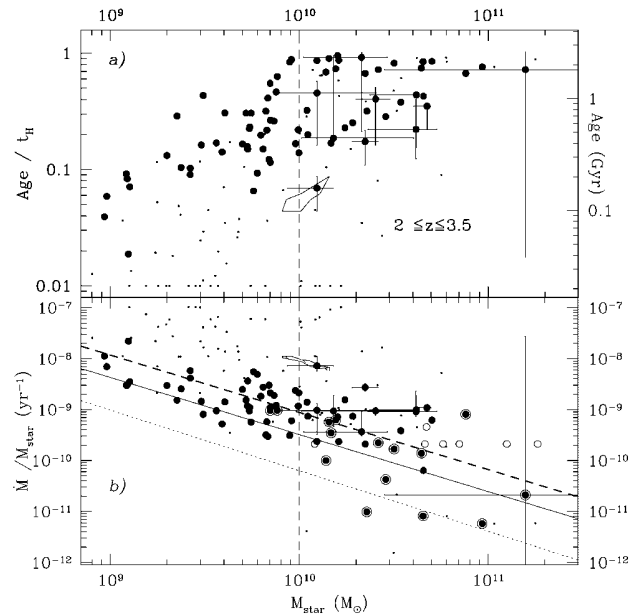

FIG. 3.—Rest-frame properties of $z > 2$ galaxies from spectral fitting of the HDF-S sample. The vertical dashed line shows the rough estimated limit for mass completeness in the $z > 2$ sample. (*a*) Best-fit age (divided by the corresponding Hubble time) as a function of stellar mass. For comparison, we show in the right vertical axis the corresponding ages at $z = 2.5$. (*b*) Specific star formation rate as a function of stellar mass, compared with the average relations at $0.2 < z < 0.5$ (*thin dotted line*) and at $0.75 < z < 1$ (*solid line*) from Brinchmann & Ellis (2000). The thick dashed line corresponds to our fit to the whole SMC sample. In both cases, filled dots represent the SMC-based estimates, small dots the Calzetti ones. Encircled points represent the objects with $J-K \geq 1.34$ discussed by Franx et al. (2003). Error bars are shown for a few objects, for the SMC case only; the large error bars on the most massive objects reflect the ambiguity in its nature, between passively fading and dusty star-forming objects. Note also that errors are typically correlated, as shown by the 1 σ confidence regions shown for one of the objects. Empty points show the estimates of $\dot{M}/M_*$ when a star-forming dusty solution is forced for the objects with $\dot{M}/M_* \leq 10^{-10}$ yr^{-1}; in this case the objects are fitted with slightly higher masses but without altering the order with respect to mass. [*See the electronic edition of the Journal for a color version of this figure.*]

into account that the sampling of the underlying galaxy stellar mass function may be incomplete on the massive side, because of the small HDF-S area, and may be inhomogenous at its faint side due to its varying depth as a function of z. For these reasons, we have also obtained a homogeneous estimate of its evolution computing the mass density only at 10^{10} $M_\odot \leq M_* \leq 10^{11}$ $M_\odot$ (Fig. 2, *lower panel*), where our sample is complete and well sampled at all z. This range is slightly below the typical Schechter mass in the local mass function of Cole et al. (2001). Similarly, we have also computed the same quantity in the HDF-N field, using the data of P01 and D03.

In this homogeneous subsample of relatively massive galaxies, the stellar mass density at $z > 2$ in the HDF-S is $\simeq 20^{+20}_{-5}\%$ of the local value and approaches the local one at $z \leq 1$. If we reproduce this selection criteria in our CDM model (see Fig. 2), we find that the present CDM rendition dramatically fails to reproduce the stellar mass density in massive galaxies at $z \geq 2$. Again, we find that the HDF-N is underabundant of massive galaxies with respect to HDF-S but is nevertheless well above the CDM predictions at $z \simeq 2.75$.

4. STAR-FORMING AND PASSIVE GALAXIES AT $z > 2$

We will analyze here the physical properties of the sample of $K \leq 25$ galaxies at $z_{phot} \geq 2$, which consists of 75 objects, including the 14 objects with $(J-K)_{AB} > 1.34$ emphasized by Franx et al. (2003).

First, we use the $J-K$ color to sample the amplitude of the rest-frame D4000 break, which is sensitive to the age of the stellar population We find that most of the K-selected $z \geq 2$

sample is distributed over a large range $0 < (J-K)_{AB} \leq 1.5$, suggestive of a significant spread in the stellar population ages. This is confirmed by the ages obtained from the best-fit spectral templates, which are plotted as a function of M_* in the upper panel of Figure 3. It is shown that the observed range of $J-K$ colors translates into a spread of fitted ages, ranging from 10^8 to 3×10^9 Gyr for the complete $M_* \gtrsim 10^{10}$ $M_\odot$ subsample, with about half of the sample close to the relevant Hubble time. At lower masses, the fraction of younger objects seems to increase, a result that is likely affected by the biases against old/passive low mass objects.

At the same time, we find that most of the sample is UV bright (see Poli et al. 2003, Fig. 2) and is restricted to the range of $0.1 \lesssim V-I \lesssim 0.5$, corresponding to $0.05 \lesssim E(B-V) \lesssim 0.2$ for an SMC extinction curve. We will use in the following the derived best-fit star formation rates (that include a correction for reddening), which are in agreement with those derived with a fixed conversion between the SFR and L_{1400}, assuming an $E(B-V) \simeq 0.15$.

Only seven "red" objects are detected at both large $V-I \gtrsim 1$ and $J-K \gtrsim 1.5$, a combination that may be due either to a strongly absorbed star-forming galaxy or to a passively fading stellar population, an ambiguity that cannot be safely removed without spectroscopy (Cimatti et al. 2002). For the present data set, we have found that the spectral fitting to the

complete *UBVIJHK* distribution slightly prefers the "passive" spectral model; when we force the star-forming dusty solution by selecting $\tau/\text{age} \geq 2$, we find that typical χ^2_{red}-values are larger by a factor of 2, albeit still statistically acceptable ($\chi^2_{\text{red}} \leq 1.4$).

The output of the fitting procedure is summarized in the lower panel of Figure 3, where we plot the specific star formation rate $\dot{M}/M_*$ for the *K*-selected $z > 2$ sample. At lower redshifts, the evolution of $\dot{M}/M_*$ has been studied by BE00, of which we plot in Figure 3 their average relations at $0.2 < z < 0.5$ and at $0.75 < z < 1$. They showed evidence for an increase of the average $\dot{M}/M_*$ (at a given M_*) with z; we find that the trend of increasing $\dot{M}/M_*$ with z still continues at $z \simeq 3$. A regression to our data yields $\log(\dot{M}/M_*) = 2.18 - 1.245 \log(M_*)$, i.e., the same slope but a factor of 3 higher than the $z \simeq 1$ data. At the median value of the $M_* > 10^{10}$ $M_\odot$ complete sample ($M_* = 3.2 \times 10^{10}$ $M_\odot$), the average specific star formation rate as derived from the linear interpolation is $\langle \dot{M}/M_* \rangle \simeq 4 \times 10^{-10}$ yr^{-1}. We also note that the adoption of a Calzetti extinction curve would shift this it to a much higher value of $\langle \dot{M}/M_* \rangle \simeq 2.3 \times 10^{-9}$ yr^{-1}. We have found that the average Scalo *b* parameter SFR × age/mass, as estimated from the best-fit quantities, is about 0.8 in this star-forming sample, suggesting a long duration of the starburst activity.

At the same time, we plot in Figure 3 the seven "red" objects (over 30 of the mass-complete subsample) discussed before. These objects have $\dot{M}/M_* < 10^{-10}$ yr^{-1}, i.e., more than 10 times lower that the typical $z \geq 2$ population if we adopt the "passively fading" fitting models, but follow the average trend if we adopt the "star-forming" solution. Given the ambiguity of their spectral classification, they can be used to obtain an upper limit to the fraction of galaxies that formed most of their stars in short episodes prior the time they are observed. In the HDF-S, these "passively fading" objects contribute at most to about 25% of the total number density of the mass-complete subsample of $z \simeq 3$ galaxies. In this case, the cosmological mass density due to these seven objects is 1.95×10^7 $M_\odot$ Mpc^{-3} and hence contributes up to $\simeq 40\%$ of the total mass density of the mass-complete subsample, which is 4.5×10^7 $M_\odot$ Mpc^{-3}. As can be derived from Figure 3, the mass density does not change appreciably if we assume the star-forming dusty solution for these objects.

Finally, we note that most of these "red" objects are drawn from the $(J-K)_{\text{AB}} > 1.34$ subsample discussed by Franx et al. (2003), although other objects of this class are actively star forming. The total mass density in the $(J-K)_{\text{AB}} > 1.34$ sample is 3.7×10^7 $M_\odot$ Mpc^{-3}.

5. SUMMARY

We have used new ultradeep *JHK* images of the HDF-S to trace the evolution of the stellar mass density $\rho_*(z)$ from $z \simeq 0.5$ to $z \simeq 3.5$, with the following main results:

1. We find clear evidence for a decrease of the observed stellar mass density with increasing redshifts. At $2 \leq z \leq 3.5$ the stellar mass density of both of the whole $K_{\text{AB}} \leq 25$ sample and of the homogeneous subsample of galaxies with 10^{10} $M_\odot \leq M_* \leq 10^{11}$ $M_\odot$ are about 15%–20% (with a solid upper bound of 40%) of the local value, a value 2 times higher than the analogous result in the HDF-N (Dickinson et al. 2003), and approaches the local value only at $z \simeq 1$. The UV-based cosmic star formation history (e.g., Steidel et al. 1999) reproduces the observed evolution of the total $\rho_*(z)$ (Fig. 1).

2. In the mass-limited subsample at $z > 2$, we find that the fraction of passively fading galaxies is *at most* 25%, and they can contribute up to about 40% of the measured stellar mass density.

3. Galaxies of $M_* \simeq 3 \times 10^{10}$ $M_\odot$ at $z > 2$ form stars at a specific rate of at least $\langle \dot{M}/M_* \rangle \simeq 4 \times 10^{-10}$ yr^{-1}, a value 3 times higher than what is observed at $z \leq 1$ (BE00). The inverse of this rate is the time required for these objects to double their mass, assuming constant star formation rate; in our sample, this turns out to be 2.5 Gyr, comparable both to the Hubble time of the sample and to the cosmic time up to $z = 1$. Given the high fraction of star-forming galaxies in our mass-complete sample at $z \simeq 2.5$, it is likely that their observed star formation episodes last long enough to build up a substancial fraction of the observed mass density at $z \simeq 1$.

Overall, these data suggest a scenario in which the growth of $\rho(z)$ in relatively massive galaxies is consistent with their UV-inferred star formation properties.

Finally, the large best-fit ages and Scalo *b* parameters of our $z > 2$ galaxies suggest that the global star formation rate should have been relatively high up to very high z, consistent with the results of recent searches of $z \simeq 5$–6 galaxies (e.g., Fontana et al. 2003).

At first glance, this scenario is broadly consistent with the CDM theoretical expectation, where both "quiescent" star formation rate and bursts during gas-rich mergings occur at a high rate at $z > 1$. Despite this, our rendition of CDM models largely fails to reproduce the mass density of the most massive galaxies, even if we assume the average value between HDF-N and HDF-S. Hence, the failure to reproduce the amount of baryons condensed into stars suggests that the star formation in these massive objects occurs in a more efficient fashion than what was accounted for by our recipes, as also suggested by other results directly related to the high star formation rates found at $z \geq 3$ (Fontana et al. 2003; Poli et al. 2003).

REFERENCES

Brinchmann, J., & Ellis, R. S. 2000, ApJ, 536, L77 (BE00)
Bruzual A., G., & Charlot, S. 1993, ApJ, 405, 538
Calzetti, D., et al. 2000, ApJ, 533, 68
Casertano, S., et al. 2000, AJ, 120, 2747
Cimatti, A., et al. 2002, A&A, 381, L68
Cohen, J. G. 2002, ApJ, 567, 672
Cole, S., et al. 2001, MNRAS, 326, 255
Dickinson, M., Papovich, C., Ferguson, H. C., & Budavari, T. 2003, ApJ, 587, 25 (D03)
Drory, N., et al. 2001, ApJ, 562, L111
Fontana, A., et al. 2000, AJ, 120, 2206 (F00)
———. 2003, ApJ, 587, 544
Franx, M., et al. 2003, ApJ, 587, 25

Giallongo, E., et al. 1998, AJ, 115, 2169
Kauffmann, G., et al. 2003, MNRAS, 341, 54
Labbé, I., et al. 2003, AJ, 125, 1107
Le Borgne, D., & Rocca-Volmerange, B. 2002, A&A, 386, 446
Menci, N., et al. 2002, ApJ, 575, 18
Papovich, C., Dickinson, M., & Ferguson, H. C. 2001, ApJ, 559, 620 (P01)
Poli, F., et al. 2003, ApJ, 593, L1
Saracco, P., et al. 2003, A&A, submitted
Sawicki, M., & Mallen-Ornelas, G. 2003, AJ, 126, 1208
Shapley, A. E., et al. 2001, ApJ, 562, 95
Steidel, C. C., et al. 1999, ApJ, 519, 1
Vanzella, E., et al. 2001, AJ, 122, 2190
———. 2002, A&A, 396, 847